Possible future upgrades of the direct-geometry chopper spectrometer 4SEASONS

Ryoichi Kajimoto[1,*], *Mitsutaka* Nakamura[1], *Kazuya* Kamazawa[2], *Yasuhiro* Inamura[1], *Kazuki* Iida[2], *Kazuhiko* Ikeuchi[2], and *Motoyuki* Ishikado[2]

[1]Materials and Life Science Division, J-PARC Center, Japan Atomic Energy Agency, Tokai, Ibaraki 319-1195, Japan
[2]Neutron Science and Technology Center, Comprehensive Research Organization for Science and Society, Tokai, Ibaraki 319-1106, Japan

Abstract. 4SEASONS is a direct geometry time-of-flight spectrometer installed in the Materials and Life Science Experimental Facility, the Japan Proton Accelerator Research Complex. It is used to study atomic and spin dynamics in the energy range of 10^0 meV to 10^2 meV. Since more than a decade has crossed after the first inelastic scattering experiment, it is essential to consider upgrading the instrument to improve its flexibility and performance. In this paper, we discuss the possible medium-term upgrades of key components of the instrument like the chopper system, which are achievable with the current technology and at reasonable cost. Herein, we demonstrated that 4SEASONS can improve the energy resolution by a factor of two, remove frame overlap of adjacent incident energies, significantly improve the asymmetry in the pulse shape, and increase the flux by a factor of ~1.5, without major technical difficulties.

1 Introduction

4SEASONS, also known as *SIKI*, is one of the inelastic neutron scattering instruments in the Materials and Life Science Experimental Facility (MLF) in the Japan Proton Accelerator Research Complex (J-PARC). It is a direct geometry time-of-flight spectrometer that utilizes a Fermi chopper as a monochromator to study atomic and spin dynamics in the energy range of 10^0–10^2 meV. This instrument was originally constructed for examining high-critical-temperature superconductors and was associated with high intensity and high efficiency [1]. Thus, the instrument is now considered as a middle-resolution and high-intensity spectrometer that covers the middle momentum-energy region in the inelastic/quasielastic neutron spectrometers in MLF [2–4].

The first inelastic scattering experiment using 4SEASONS was conducted in 2009 [5], and since then, its research target has been expanded to include quantum magnets, frustrated magnets, itinerant magnets, multiferroic materials, thermoelectric materials, glasses, and catalysis. Hence, this calls for serious consideration of upgrading the instrument to improve its flexibility and performance. We have made several upgrades to the instrument, such as minimizing background scattering, introducing new sample environments, filling the detector vacancy, replacing malfunctioning or aged equipment, etc. [6–11]. These short-term upgrades were undertaken as per the requirement to ensure the instrument provides its designed performance. In the present study, we discuss the possibilities of medium-term upgrades of key components of the instrument such as the chopper system. Here, we discuss the upgrades achievable using the current technology and within reasonable cost. We also focus on the effectiveness and feasibility of these upgrades in improving the performance and flexibility of the instrument. We set aside long-term upgrades requiring the redesign of the instrument from scratch or new technology currently unavailable, which will be considered in the future accompanying an upgrade of the whole MLF or construction of the second target station.

2 Instrument layout

Figure 1 shows the schematic top and side views of 4SEASONS [1]. 4SEASONS is located at the beamline 1 (BL01) viewing the coupled moderator [12]. The sample is located at L_1 = 18 m from the moderator. The supermirror-coated guide is placed between the 2.3 m and 15.8 m positions to minimize the loss of neutrons during the beam transport. It has an elliptically converging shape with one of the focal points being located at the sample. The incident neutron beam transported by the neutron guide is monochromatized by the Fermi chopper. It is located at L_3 = 1.7 m upstream of the sample and rotates at 600 Hz at maximum. The scattered neutrons are detected at 3/4-in-diameter and 2.5-m-long position-sensitive detectors (PSDs) surrounding the sample cylindrically at a distance of L_2 = 2.5 m from −35° to +130° with respect to the incident beam. The PSDs are ^{3}He tubes with a ^{3}He partial pressure of 16 atm. In addition to the Fermi chopper, 4SEASONS has a T_0 chopper and two disk choppers. The T_0 chopper rotates at 100 Hz at maximum and is placed

*e-mail: ryoichi.kajimoto@j-parc.jp

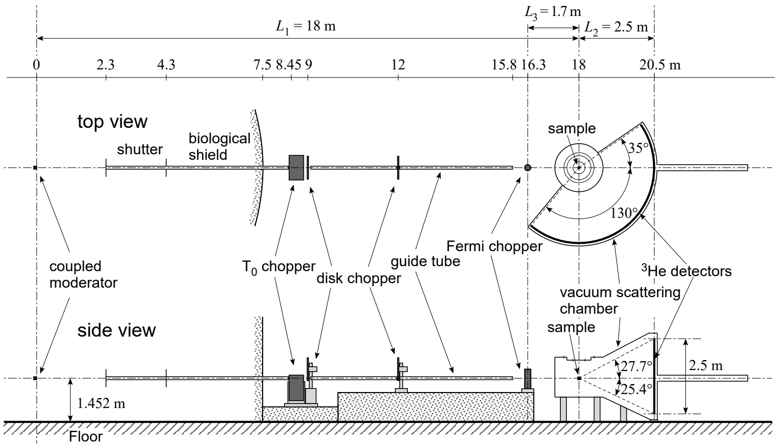

Figure 1. Layout of 4SEASONS [1].

at 8.45 m from the moderator. It is used to suppress the prompt pulse. On the other hand, the two disk choppers are installed at 9 m and 12 m and rotate at 12.5 Hz or 25 Hz. These two choppers are used to define the usable incident energy band and to eliminate the frame overlaps of very low energy neutrons.

3 Candidates of upgrade items

3.1 Fermi chopper and optimum resolution

The Fermi chopper of 4SEASONS utilizes straight-slit package. This package is advantageous in multi-E_i measurements using the repetition rate multiplication (RRM) [5, 13–15] because of the equal transmissions at the $2n\pi$ and $(2n+1)\pi$ rotations (n is integer). The ratio of the width (w) to the length (D) of each slit is 0.02 [16]. The parameters of the slit package were designed to produce approximately 5% energy resolution at elastic scattering under the "optimum" condition in which the chopper opening time Δt_{ch} is equal to the moderator pulse width Δt_m, i.e., $\Delta t_{ch} = \Delta t_m$ [1, 17, 18] [Fig. 2(a)]. The above condition can be fulfilled at E_i below 500 meV by considering that the minimum of Δt_{ch} is 5.3 μs in full width at half maximum (FWHM) at 600 Hz rotation [Fig. 2(b)]. This E_i is sufficient to cover the target dynamic range of the instrument.

However, the energy resolution at low energy transfers may be insufficient with the above condition. This is because the contribution of the Fermi chopper to energy resolution increases substantially at low energy transfers [19, 20]. This further limits the usability of the instrument, even though the low energy transfer region can be covered by lower E_is available via the RRM. It is likely that the above condition was too naïve for 4SEASONS, and we should reconsider the optimum condition for low energy transfers based on the idea that the Fermi chopper contributes to the energy resolution similarly to others [21].

The resolution of the energy transfer relative to E_i is given by [22]:

$$\left(\frac{\Delta E}{E_i}\right)^2 = \left\{2\frac{\Delta t_{ch}}{t_{ch}}\left[1+\frac{L_1}{L_2}\left(\frac{E_f}{E_i}\right)^{\frac{3}{2}}\right]\right\}^2 + \left\{2\frac{\Delta t_m}{t_{ch}}\left[1+\frac{L_3}{L_2}\left(\frac{E_f}{E_i}\right)^{\frac{3}{2}}\right]\right\}^2 + \left[2\frac{\Delta L_2}{L_2}\left(\frac{E_f}{E_i}\right)\right]^2, \quad (1)$$

where ΔL_2 is the uncertainty of L_2 because of the sample and the detector sizes. Let us neglect the contribution from ΔL_2 for simplicity because it is independent of Δt_{ch} and Δt_m. Equating the Δt_{ch} and Δt_m terms in Eq. (1) leads the following optimum condition as shown in literature [21, 23],

$$\frac{\Delta t_{ch}}{\Delta t_m} = 1 - \frac{L_{ch}}{L_1 + L_2(E_i/E_f)^{3/2}}, \quad (2)$$

where L_{ch} is the distance between the moderator and the Fermi chopper ($L_{ch} = L_1 - L_3$). The condition $\Delta t_{ch} = \Delta t_m$ corresponds to the extreme case when E is its maximum, E_i. However, for general cases, Eq. (2) is less than unity, and it becomes

$$\Delta t_{ch} = \frac{L_2 + L_3}{L_1 + L_2}\Delta t_m, \quad (3)$$

when $E = 0$. Eq. (3) becomes $0.20\Delta t_m$ with $L_1 = 18$ m, $L_2 = 2.5$ m, and $L_3 = 1.7$ m.

Figure 2(a) shows energy resolutions as a function of E_i calculated using the moderator pulse width of BL01 [24] and Eq. (1) by varying Δt_{ch} from Δt_m to $0.1\Delta t_m$. The increase below $E_i \sim 50$ meV is due to the broadening of the pulse width of the coupled moderator, while $\Delta E/E_i$ is almost constant above this energy because Δt_m is proportional to $E_i^{-1/2}$ [25]. The energy resolution for $\Delta t_{ch} = \Delta t_m$ becomes 5%–6% above ~50 meV as designed. By decreasing Δt_{ch}, the energy resolution smoothly decreases. With $\Delta t_{ch} = 0.2\Delta t_m$, we can obtain less than 3% resolution above 20 meV, and 4% resolution even at 10 meV. Such values of resolutions are comparable with those of

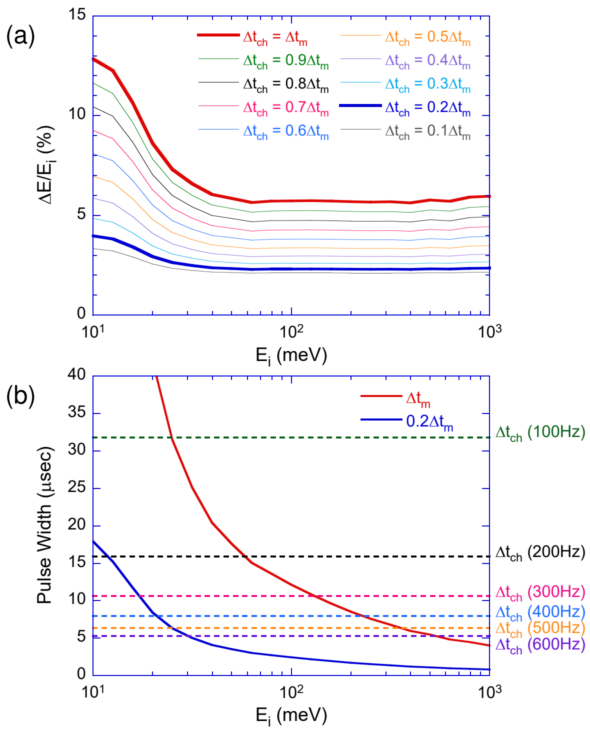

Figure 2. (a) Calculated energy resolutions as a function of E_i when Δt_ch varies from Δt_m to $0.1\Delta t_\mathrm{m}$. The cases of $\Delta t_\mathrm{ch} = \Delta t_\mathrm{m}$ and $0.2\Delta t_\mathrm{m}$ are indicated by thick lines. The sample size is 20 mm in diameter. (b) The moderator pulse width of BL01 Δt_m and $0.2\Delta t_\mathrm{m}$ as a function of E_i. Broken lines indicate the chopper pulse width for the 4SEASONS Fermi chopper rotated at 100–600 Hz.

existing chopper spectrometers and are good enough for a middle-resolution and high-intensity spectrometer like 4SEASONS. It should be noted that the improvement in the resolution slows down with decreasing Δt_ch and becomes almost saturated at $\Delta t_\mathrm{ch} < 0.2\Delta t_\mathrm{m}$. This is because the resolution is dominated by contributions other than the Fermi chopper at such a small Δt_ch.

Figure 2(b) shows the moderator pulse width in FWHM and the one multiplied by 0.2 together with the chopper pulse widths obtained from the present Fermi chopper for several rotation speeds. The condition of $\Delta t_\mathrm{ch} = 0.2\Delta t_\mathrm{m}$ can be achieved only below $E_\mathrm{i} \sim 30$ meV using the present Fermi chopper whose maximum rotation speed is 600 Hz. Since it may be technically difficult to increase the maximum rotation speed, we should introduce a new Fermi chopper with a finer slit package to overcome the limitation of Δt_ch. For example, if we employ the slit package whose w/D is half of the present value, i.e., $w/D = 0.01$, the condition of $\Delta t_\mathrm{ch} = 0.2\Delta t_\mathrm{m}$ is available up to about 100 meV. This value of w/D is feasible because Fermi choppers with a similar value [26] or even a finer value of w/D [27] are actually used. Figure 3 shows how the fine slit package improves the energy resolution. The energy-transfer spectra are compared with $w/D = 0.02$ and 0.01 when the Fermi chopper is rotated at its maximum speed of 600 Hz. The data were obtained by Monte Carlo simulation using the ray-trace simulation package McStas [28–32]. $\Delta E/E_\mathrm{i}$ estimated by the FWHMs are

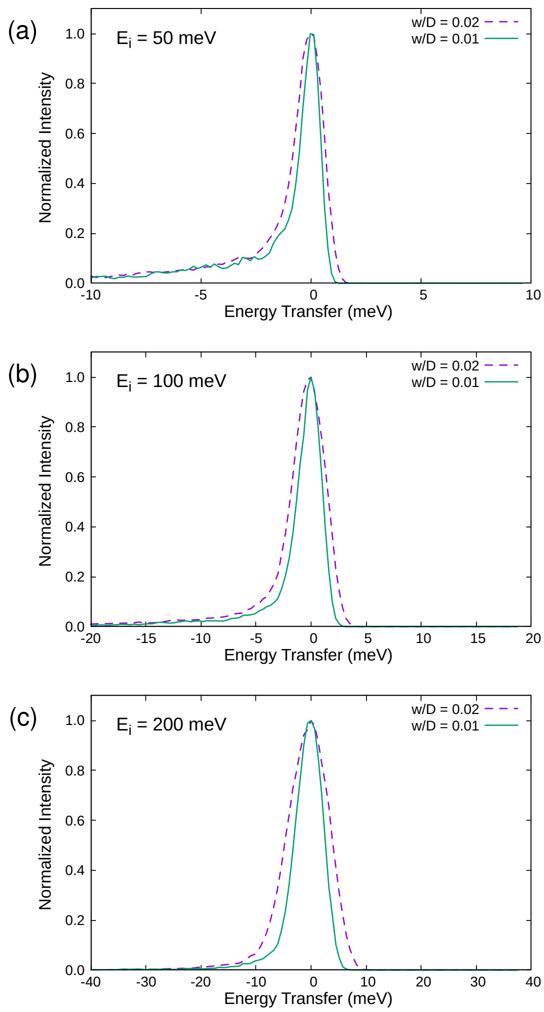

Figure 3. Energy-transfer spectra for $w/D = 0.02$ (broken lines) and 0.01 (solid lines) obtained by Monte Carlo simulations for (a) $E_\mathrm{i} = 50$ meV, (b) 100 meV, and (c) 200 meV. The Fermi chopper with D = 20 mm is rotated at 600 Hz. The sample is a 1-mm thick hollow cylindrical vanadium that is 20 mm in diameter and 20 mm in height. The peak intensities are normalized to unities.

3.1%, 3.6%, and 4.4% for E_i = 50, 100, and 200 meV, respectively, when $w/D = 0.02$. When $w/D = 0.01$, the estimated $\Delta E/E_\mathrm{i}$ reduce to 2.1%, 2.5%, and 2.9%, respectively. These results are consistent with the analytical estimation in Fig. 2. About 70% reduction of the resolution is significant, but the use of fine slits and high rotation speed of the Fermi chopper reduce the neutron transmission. This loss in neutron flux can be compensated by adopting curved slits. The curved slits will be less efficient in multi-E_i measurements because of low transmissions at the $(2n+1)\pi$ positions. Thus, the combination of the present sloppy straight-slit Fermi chopper and a new fine curved-slit Fermi chopper should be considered to be used in 4SEASONS to improve its flexibility.

3.2 Suppression of frame overlaps of incident pulses

One of the most important features of 4SEASONS is the simultaneous utilization of multiple E_is via RRM by the Fermi chopper. In recent years, this feature has become the standard for direct-geometry chopper spectrometers [23, 33–40]. However, the overlap of scattering from the adjacent E_i may limit the usable energy-transfer range, particularly at low E_is. Suppose we choose $E_i = 200$ meV and subsidiary E_is as typical experimental condition at 4SEASONS while rotating the Fermi chopper at 300 Hz. Then, this results in a series of $E_i = 200$, 75.1, 39.0, 23.9, and 16.1 meV. If we calculate the maximum energy transfer E_{clean} below which scattering from the next lower E_i never overlaps [5], E_{clean}/E_i becomes 95%, 87%, 75%, 59%, and 40%, respectively. It is known that the intensity of up-scattering from the next lower E_i drastically decreases as its energy transfer decreases toward $-\infty$ following the Bose population factor $n(E,T) = [\exp(E/k_BT) - 1]^{-1}$, where k_B and T are the Boltzmann constant and temperature, respectively. Thus, the usable energy transfer range can be enlarged, particularly at low temperatures. However, the above example has clearly shown that the overlaps of incident pulses becomes a serious problem for $E_i \sim 10$ meV or lower. To mitigate this problem, the new direct-geometry chopper spectrometers are equipped with pulse-removal choppers to control spacings between incident pulses. These pulse-removal choppers are usually disk choppers that are placed either adjacent to [23, 35–37] or away from the monochromatizing choppers [38–40]. However, 4SEASONS, which is one of the first chopper spectrometers to implement the RRM capability [5], does not have choppers dedicated for such a purpose, though it can select a single E_i by combining the opening times of the two band choppers.

In this study, we briefly discuss the feasibility of adding a pulse-removal chopper to 4SEASONS. Since the pulse-removal chopper thins out the incident pulses defined by the monochromatizing chopper, it has more advantages when placed closer to the Fermi chopper. However, the spatial constraint and the possibility of using the chopper as a pulse-shaping chopper, which will be discussed in the next subsection, need to be taken into consideration. Thus, we suggest the chopper to be placed at half of the distance between the moderator and the Fermi chopper. Figure 4 shows the cutaway view of a part of 4SEASONS near the T_0 chopper and the first disk chopper. The position at $L_{ch}/2 = 8.15$ m is marked by a down arrow. A chopper can be installed at this position without disturbing the existing choppers if the short section of the neutron guide is removed or replaced. In our case, the pulse-removal chopper can remove each second pulse if its opening period τ is the same as that of the Fermi chopper. For the straight-slit Fermi chopper rotating at 600 Hz, the required minimum opening period is 1/1200 s. The maximum rotating speed of a typical disk chopper is about 300 Hz. So, $\tau = 1/1200$ s can be achieved if we use a disk with four equally spaced apertures. On the other hand, a disk chopper with unequally spaced apertures [36, 40] or that with two disks rotating at different speeds [35] provides uneven elimination of E_is. The latter type of disk chopper also needs to be considered in the case of selectively removing low E_is with more serious frame overlap.

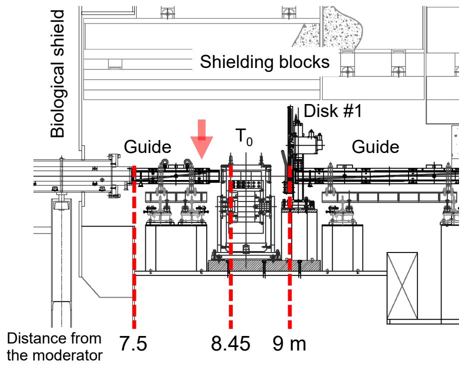

Figure 4. Cutaway view of 4SEASONS after the biological shield. “Guide,” “T_0,” and “Disk #1” denote parts of the neutron guide, the T_0 chopper, and the first disk chopper, respectively. The arrow indicates the candidate position of the pulse-removal chopper.

3.3 Pulse shaping

We have confirmed the feasibility of adding a chopper at the $L_{ch}/2$ position. Next, we discuss whether this chopper can also be used for pulse shaping. The pulse-shaping chopper is mainly used for two purposes. One purpose is to obtain a finer energy resolution by sharpening the neutron pulse width prior to the monochromatization with the Fermi chopper. The other purpose is to cut the pulse tail to improve the symmetry in the pulse shape.

In order to obtain a finer energy resolution, the opening time of the pulse-shaping chopper Δt_{ps} must be in the same order as that of the moderator pulse width. In quantitative terms, the time width at the moderator defined by the pulse-shaping chopper and the monochromatizing chopper is

$$\Delta t_m^{ch+ps} = \frac{L_{ch}}{L_{ch} - L_{ps}} \Delta t_{ps} + \frac{L_{ps}}{L_{ch} - L_{ps}} \Delta t_{ch},$$

where L_{ps} is the distance of the pulse-shaping chopper from the moderator [33]. The Δt_m^{ch+ps} should be similar to or less than Δt_m to effectively control the energy resolution by the pulse-shaping chopper. If $L_{ps} = L_{ch}/2$, Δt_{ps} must be less than $\Delta t_m/2$ even for the limiting case of $\Delta t_{ch} = 0$. The beam width at the candidate position of the pulse-shaping chopper ($L_{ps} = 8.15$ m) is ~80 mm. In the case of a typical fast-rotating disk chopper having 300 mm radius at the beam center, 80 mm slit width, and 300 Hz rotation speed, Δt_{ps} of this chopper becomes 141 μs. If we use a disk chopper with two counter-rotating disks, Δt_{ps} becomes 70 μs at most. In any case, Δt_{ps} is larger than Δt_m in most of the energy range of 4SEASONS [see Fig. 2(b)]. Therefore, This type of the pulse-shaping chopper cannot be used to obtain finer energy resolution. A narrow-slit disk chopper or a Fermi chopper can achieve sharper Δt_{ps}. However, such choppers are associated with significant loss in neutron flux. 4SEASONS can potentially achieve 2.5%–3% resolution, as discussed in §3.1, without the pulse-shaping chopper. Higher resolution should be left to other high-resolution spectrometers in MLF, such as HRC and AMATERAS.

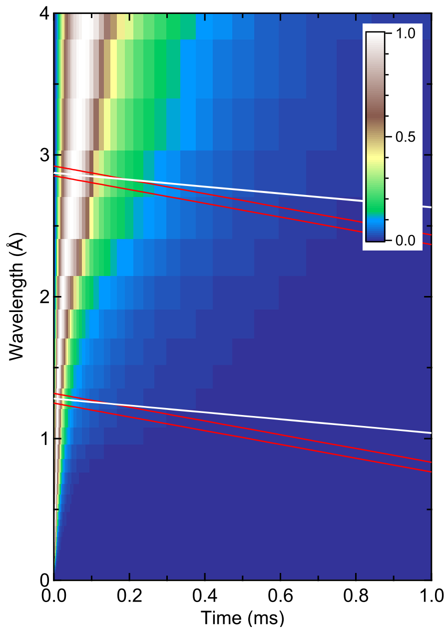

Figure 5. Time-wavelength acceptance diagram of the pulse-shaping chopper (red lines) and the Fermi chopper (white lines) for 10 meV and 50 meV neutrons. The rotation speed of the pulse-shaping chopper is 300 Hz, while that of the Fermi chopper is 200 Hz (10 meV) and 300 Hz (50 meV), respectively. Color map shows the time structure of the moderator at BL01, whose peak intensity is normalized to unity.

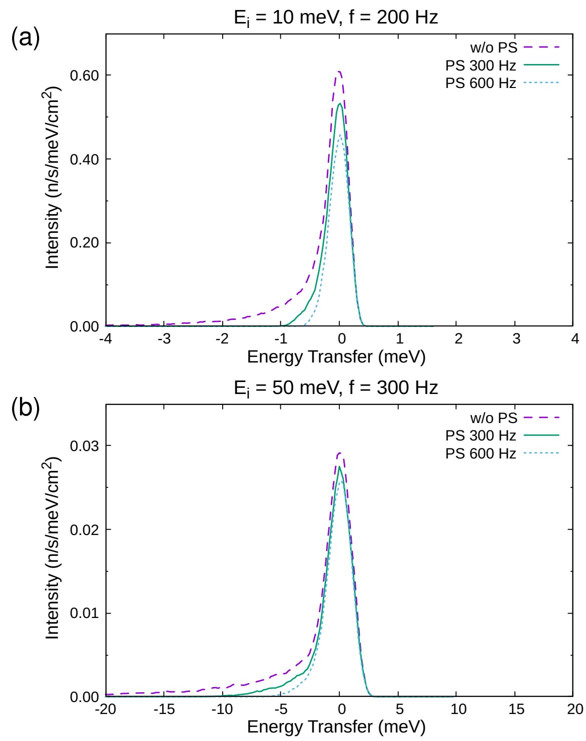

Figure 6. Energy-transfer spectra without and with the pulse shaping chopper obtained by Monte Carlo simulations. The sample is the same vanadium as used in the calculations of Fig. 3. (a) E_i = 10 meV and f = 200 Hz. (b) E_i = 50 meV and f = 300 Hz. Broken, solid, and dotted lines denote spectra without the pulse-shaping chopper, with the pulse-shaping chopper rotating at 300 Hz and at 600 Hz, respectively.

Conversely, the required conditions for Δt_ps should be mitigated for the tail cutter. The pulse tail is particularly prominent at $E_\mathrm{i} \lesssim 50$ meV where the pulse width of the coupled moderator is enhanced. The tail hampers the quantitative analysis of the observed spectra irrespective of nominal energy resolutions in, for example, quantitative estimation of line width or observation of spin gap. Therefore, suppressing the pulse tail by the pulse-shaping chopper will be useful even if the nominal energy resolution is not improved.

We plot a time-wavelength acceptance diagram in Fig. 5, following Refs. [23, 41], to examine whether the pulse-shaping chopper can cut the pulse tail effectively. Red and white lines indicate the time-wavelength regions of neutrons at the moderator that pass through the pulse-shaping chopper and the Fermi chopper, respectively. We plot the cases for 10 meV (2.9 Å) and 50 meV (1.3 Å) neutrons. The pulse-shaping chopper has a 300-mm radius and an 80 mm-wide slit as discussed above, and its rotation speed is 300 Hz. The color map in Fig. 5 shows the pulse structure of the moderator at BL01. Here, Δt_m is 90 μs and 18 μs at E_i = 10 meV and 50 meV, respectively. Figure 5 indicates that the pulse-shaping chopper can substantially cut the pulse tail for 10 meV neutrons, though the pulse-shaping chopper is less effective for 50 meV or higher-energy neutrons due to the sharp moderator pulse width. We, thus, conducted a Monte Carlo simulation study using McStas. Figure 6 shows simulated energy-transfer spectra for E_i = 10 meV and 50 meV at the detector. The rotation speeds of the Fermi chopper f were chosen to be 200 Hz and 300 Hz for E_i = 10 meV and 50 meV, respectively, so that the energy resolutions $\Delta E/E_\mathrm{i}$ became about 5%. The short guide section at ~8 m was removed to place the pulse-shaping chopper (see Fig. 4). Without the pulse-shaping chopper, the spectra show significant tails in the energy gain ($E < 0$) sides. The rotation of the pulse-shaping chopper at 300 Hz results in a finite decrease in the tails. In particular, the impact of the pulse-shaping chopper is evident at E_i = 10 meV [Fig. 6(a)]. The peak intensity slightly decreases by pulse-shaping, but it is acceptable. If we can rotate the pulse-shaping chopper at 600 Hz, the tail is significantly suppressed even at E_i = 50 meV [Fig. 6(b)]. Such a high rotation speed is not feasible with the currently available disk chopper, but a counter-rotating double-disk chopper can effectively achieve this speed. The tail cut by the pulse-shaping chopper becomes more effective at lower E_is where the moderator pulse width becomes broader, while it is less effective at E_i higher than 50 meV. However, the pulse tail becomes less prominent at high energies because of the decrease in the moderator pulse width (Fig. 3). Therefore, we conclude that the pulse-shaping chopper in 4SEASONS is effective.

3.4 Beam transport

The upgrades discussed above focused mainly on improving the resolution or pulse shape. However, these upgrades

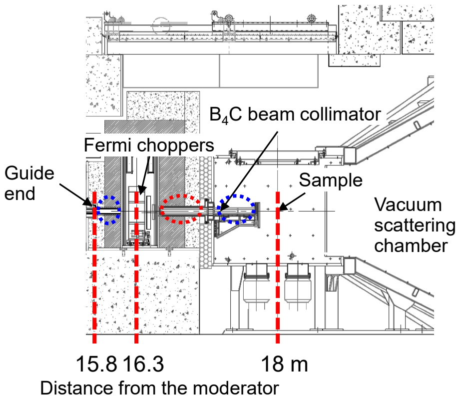

Figure 7. Cutaway view of 4SEASONS around the sample, Fermi chopper, and the end of the neutron guide. The sections marked by blue and red dotted circles are beam collimators made of B_4C (see text for details).

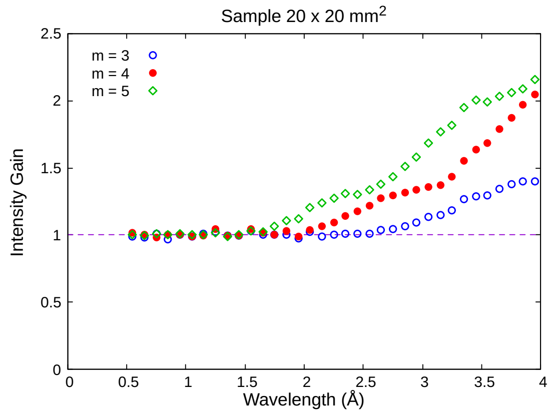

Figure 8. Gain in flux at a 20 mm × 20 mm sample by replacing the 50 mm × 50 mm × 580 mm beam collimator after the Fermi chopper with a supermirror neutron guide obtained by Monte Carlo simulation. Open circles, closed circles, and open diamonds show the gains when the *m* values of the supermirror are 3, 4, and 5, respectively.

generally decrease the neutron flux on the sample in compensation for the better pulse shape. Here, we discuss a possible upgrade of the beam transport to increase the neutron flux.

The current neutron guide is designed to transport high neutron flux at the sample [42]. It has an elliptically converging shape and uses high-critical-angle supermirrors whose *m* values are 3.2–4 (*m* is the critical angle relative to that of the nickel mirror). Given the relatively short flight path to the sample, modifying the design of the existing guide will not be effective in increasing the neutron flux.

On the other hand, 4SEASONS still has a room for extending the neutron guide. Figure 7 shows a cutaway view of 4SEASONS at the end of the neutron guide and the sample position. The neutron guide ended 0.5 m before the Fermi chopper, resulting in a substantially large space between the Fermi chopper and the sample. This space is left for future upgrade, and beam collimators made of B_4C are currently installed. Thus, the neutron guide can be extended by about 1 m. Currently, the total length of the neutron guide, excluding the length of gaps for the choppers, is about 12.7 m. The total flight path between the moderator and the sample *without* the neutron guide is 18 m − 12.7 m = 5.3 m. If the flight path with the neutron guide is extended by 1 m, the flight path without the neutron guide becomes 4.3 m. Suppose the neutron guide transports neutrons by 100% for simplicity, then we need to consider only the flight path without the neutron guide. Thus, a rough estimate of the flux gain becomes $(5.3\,\mathrm{m}/4.3\,\mathrm{m})^2 = 1.5$. The 50% increase in flux is significant and should be examined in detail.

Figure 8 shows a more practical study of the gain by extending the neutron guide. We assumed that the 50 mm × 50 mm × 580 mm beam collimator placed after the Fermi chopper (indicated by a red dotted circle in Fig. 7) was replaced with a supermirror-coated neutron guide having the same dimension. Thus, the gain in intensity at a 20 mm × 20 mm sample was calculated by Monte Carlo simulation using McStas. By adding only this short neutron guide, we obtained a positive result. If we use the $m = 4$ supermirror, which is the same as that used in the downstream part of the present neutron guide, we can obtain a finite gain at a wavelength longer than 2 Å (∼20 meV), and the gain reaches about two at 4 Å (∼5 meV). Recently an *m* value higher than 5 is commercially available; this will be beneficial for shorter wavelengths. If the sample size is larger, then the gain at short wavelengths will be larger, while the gain at long wavelengths will be enhanced by utilizing a focusing shape. Thus, there is a need for a more detailed analytical and numerical study to optimize the specifications of the extended guide.

3.5 Flight paths

In the previous sections, we have discussed practical upgrades without changing the key flight paths of L_1, L_2, and L_3. This is because the modification of these flight paths requires complete redesigning of the instrument, which is out of the scope of the present paper. Nevertheless, understanding how changes in flight paths affect the performance of the instrument will help in preparing for future major upgrades or development of a new spectrometer. To finish this paper, we briefly discuss this issue in terms of the energy resolution.

The energy resolution of the direct-geometry chopper spectrometer improves with the increase in L_1 and L_2 and the decrease in L_3. However, the contribution of L_1 saturates as L_1 increases [see Eq. (1)], and L_1 longer than ∼15 m is not advantageous to the energy resolution at short-pulse facilities, including J-PARC [17, 43]. Figure 9(a) shows calculated energy resolutions as a function of the energy transfer for $L_1 = 18$ m, 20 m, and 30 m when $E_i = 50$ meV and $f = 300$ Hz. Even if L_1 is extended by 12 m, the energy resolution will improve by only 0.5% at elastic scattering. Similarly, shortening L_3 shows little improvement in energy resolution, as shown in Fig. 9(c). If L_3 is reduced to 1 m, which is the practical minimum value

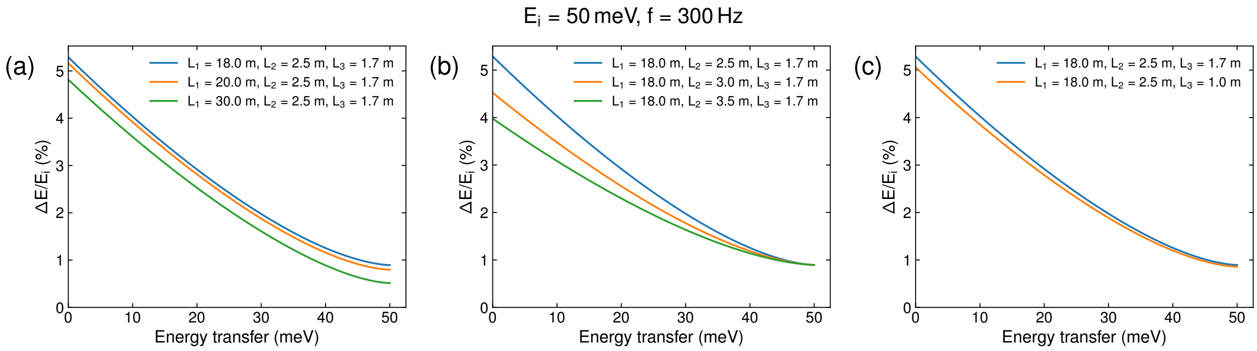

Figure 9. Calculated energy resolutions as a function of energy transfer for several sets of flight paths. E_i, f, and the sample diameter are 50 meV, 300 Hz, and 20 mm, respectively. (a) The case varying L_1 as 18 m, 20 m, and 30 m with L_2 and L_3 being fixed at 2.5 m and 1.7 m, respectively. (b) The case varying L_2 as 2.5 m, 3.0 m, and 3.5 m with L_1 and L_3 being fixed at 18 m and 1.7 m, respectively. (c) The case varying L_3 as 1.7 m and 1.0 m with L_1 and L_2 being fixed at 18 m and 2.5 m, respectively.

considering the required space for sample environment devices, the energy resolution will improve by only 0.2% at elastic scattering. Conversely, lengthening L_2 is the most effective way to improve energy resolution. As shown in Fig. 9(b), increasing L_2 by only 0.5 m improves the energy resolution by 0.8% at elastic scattering. In reality, the flight paths are limited by spatial constraints as long as 4SEASONS continues to reside at BL01. However, L_2 can be extended by ~0.5 m and should be considered when reconstructing the vacuum scattering chamber in the future.

4 Conclusion

In this paper, we discuss the possible upgrades of the key components of 4SEASONS to examine their feasibility in improving the performance and flexibility of the instrument. We demonstrated that 4SEASONS can improve the energy resolution by a factor of two, remove frame overlap of adjacent incident energies, significantly improve asymmetry in the pulse shape, and increase the flux by a factor of ~1.5, without major technical difficulties. The findings of this study will contribute to the development of future upgrades for the 4SEASONS spectrometer. More detailed quantitative studies, including numerical simulations and prioritization based on scientific needs, budget, and human resources, are required to further elucidate the proposed upgrades.

We thank the members of the MLF Spectroscopy Group for valuable discussions. This work was supported by JSPS KAKENHI Grant Numbers 19K12648 and 22K12663.

References

[1] R. Kajimoto, M. Nakamura, Y. Inamura, F. Mizuno, K. Nakajima, S. Ohira-Kawamura, T. Yokoo, T. Nakatani, R. Maruyama, K. Soyama et al., J. Phys. Soc. Jpn. **80**, SB025 (2011)

[2] H. Seto, S. Itoh, T. Yokoo, H. Endo, K. Nakajima, K. Shibata, R. Kajimoto, S. Ohira-Kawamura, M. Nakamura, Y. Kawakita et al., Biochim. Biophys. Acta, Gen. Subj. **1861**, 3651 (2017)

[3] K. Nakajima, Y. Kawakita, S. Itoh, J. Abe, K. Aizawa, H. Aoki, H. Endo, M. Fujita, K. Funakoshi, W. Gong et al., Quantum Beam Sci. **1**, 9 (2017)

[4] R. Kajimoto, T. Yokoo, M. Nakamura, Y. Kawakita, M. Matsuura, H. Endo, H. Seto, S. Itoh, K. Nakajima, S. Ohira-Kawamura, Physica B **562**, 148 (2019)

[5] M. Nakamura, R. Kajimoto, Y. Inamura, F. Mizuno, M. Fujita, T. Yokoo, M. Arai, J. Phys. Soc. Jpn. **78**, 093002 (2009)

[6] R. Kajimoto, M. Nakamura, Y. Inamura, K. Ikeuchi, S. Ji, K. Nakajima, S. Ohira-Kawamura, W. Kambara, M. Sawabe, A. Kamiya et al., J. Phys. Soc. Jpn. **82**, SA032 (2013)

[7] M. Nakamura, Y. Kawakita, W. Kambara, K. Aoyama, R. Kajimoto, K. Nakajima, S. Ohira-Kawamura, K. Ikeuchi, T. Kikuchi, Y. Inamura et al., JPS Conf. Proc. **8**, 036011 (2015)

[8] R. Kajimoto, M. Nakamura, Y. Inamura, K. Kamazawa, K. Ikeuchi, K. Iida, M. Ishikado, K. Nakajima, S. Ohira-Kawamura, T. Nakatani et al., in *Proc. ICANS-XXI* (2015), JAEA-Conf 2015-002/KEK Proceedings 2015-7, p. 319

[9] M. Nakamura, W. Kambara, K. Iida, R. Kajimoto, K. Kamazawa, K. Ikeuchi, M. Ishikado, K. Aoyama, Physica B **551**, 480 (2018)

[10] R. Kajimoto, M. Nakamura, Y. Inamura, K. Kamazawa, K. Ikeuchi, K. Iida, M. Ishikado, N. Murai, H. Kira, T. Nakatani et al., J. Phys.: Conf. Ser. **1021**, 012030 (2018)

[11] R. Kajimoto, M. Ishikado, H. Kira, K. Kaneko, M. Nakamura, K. Kamazawa, Y. Inamura, K. Ikeuchi, K. Iida, N. Murai et al., Physica B **556**, 26 (2019)

[12] H. Takada, K. Haga, M. Teshigawara, T. Aso, S. Meigo, H. Kogawa, T. Naoe, T. Wakui, M. Ooi, M. Harada et al., Quantum Beam Sci. **1**, 8 (2017)

[13] F. Mezei, J. Neutron Res. **6**, 3 (1997)

[14] F. Mezei, M. Russina, S. Schorr, Physica B **276-278**, 128 (2000)

[15] M. Russina, F. Mezei, Nucl. Instrum. Methods Phys. Res., Sect. A **604**, 624 (2009)
[16] M. Nakamura, R. Kajimoto, JPS Conf. Proc. **1**, 014018 (2014)
[17] S. Itoh, M. Arai, T. Otomo, K. Ohoyama, T. Osakabe, K. Kuwahara, J. Suzuki, M. Matsuda, KEK Report 2001-3 (2001)
[18] S. Itoh, T. Yokoo, S. Satoh, S. Yano, D. Kawana, J. Suzuki, T.J. Sato, Nucl. Instrum. Methods Phys. Res., Sect. A **631**, 90 (2011)
[19] M. Arai, R. Kajimoto, M. Nakamura, Y. Inamura, K. Nakajima, K. Shibata, N. Takahashi, J. Suzuki, S. Takata, T. Yamada et al., J. Phys. Soc. Jpn. **82**, SA024 (2013)
[20] R. Kajimoto, M. Nakamura, K. Iida, K. Kamazawa, K. Ikeuchi, Y. Inamura, M. Ishikado, J. Neutron Res. **22**, 99 (2020)
[21] R.E. Lechner, in *Proc. ICANS-XI* (1991), KEK Report 90-25, p. 717
[22] C.G. Windsor, *Pulsed Neutron Scattering* (Taylor & Francis Ltd., London, 1981)
[23] J. Voigt, N. Violini, T. Brückel, Nucl. Instrum. Methods Phys. Res., Sect. A **741**, 26 (2014)
[24] `http://j-parc.jp/researcher/MatLife/en/instrumentation/ns3.html`
[25] D. Mildner, R. Sinclair, Ann. Nucl. Energy **6**, 225 (1979)
[26] S. Itoh, T. Yokoo, T. Masuda, S. Asai, H. Saito, D. Kawana, R. Sugiura, T. Asami, Y. Ihata, Physica B **568**, 76 (2019)
[27] J.Y. Lin, A. Banerjee, F. Islam, M.D. Le, D.L. Abernathy, Physica B **562**, 26 (2019)
[28] K. Lefmann, K. Nielsen, Neutron News **10**, 20 (1999)
[29] P. Willendrup, E. Farhi, K. Lefmann, Physica B **350**, E735 (2004)
[30] P. Willendrup, E. Farhi, E. Knudsen, U. Filges, K. Lefmann, J. Neutron Res. **17**, 35 (2014)
[31] P.K. Willendrup, K. Lefmann, J. Neutron Res. **22**, 1 (2020)
[32] P.K. Willendrup, K. Lefmann, J. Neutron Res. **23**, 7 (2021)
[33] K. Nakajima, S. Ohira-Kawamura, T. Kikuchi, M. Nakamura, R. Kajimoto, Y. Inamura, N. Takahashi, K. Aizawa, K. Suzuya, K. Shibata et al., J. Phys. Soc. Jpn. **80**, SB028 (2011)
[34] G. E. Granroth, J. Phys. Soc. Jpn. **80**, SB016 (2011)
[35] P. Deen, A. Vickery, K. Andersen, R. Hall-Wilton, EPJ Web Conf. **83**, 03002 (2015)
[36] G. Sala, J.Y.Y. Lin, V.B. Graves, G. Ehlers, J. Appl. Crystallogr. **51**, 282 (2018)
[37] P.P. Deen, S. Longeville, W. Lohstroh, F. Moreira, G. Fabrèges, L. Loaiza, D. Noferini, Rev. Sci. Instrum. **92**, 105104 (2021)
[38] R. Bewley, J. Taylor, S. Bennington., Nucl. Instrum. Methods Phys. Res., Sect. A **637**, 128 (2011)
[39] M. Russina, G. Guenther, V. Grzimek, R. Gainov, M.C. Schlegel, L. Drescher, T. Kaulich, W. Graf, B. Urban, A. Daske et al., Physica B **551**, 506 (2018)
[40] R.A. Ewings, J.R. Stewart, T.G. Perring, R.I. Bewley, M.D. Le, D. Raspino, D.E. Pooley, G. Škoro, S.P. Waller, D. Zacek et al., Rev. Sci. Instrum. **90**, 035110 (2019)
[41] K.H. Andersen, J. Neutron Res. **10**, 179 (2002)
[42] R. Kajimoto, K. Nakajima, M. Nakamura, K. Soyama, T. Yokoo, K. Oikawa, M. Arai, Nucl. Instrum. Methods Phys. Res., Sect. A **600**, 185 (2009)
[43] K. Ohoyama, S. Itoh, T. Otomo, T. Osakabe, J. Suzuki, M. Matsuda, K. Kuwahara, M. Arai, in *Proc. ICANS-XV* (2001), JAERI-Conf 2001-002/KEK Proceedings 2000-22, p. 418